EFFECT OF PARTICLE SIZE ON THE MAGNETIC PROPERTIES OF BARIUM HEXAFERRITE BONDED MAGNETS

Thesis Submitted in Partial fulfilment of the requirement for

The award of the degree of

Master of Technology (M.Tech.)

In

MATERIALS AND METALLURGICAL ENGINEERING

Submitted by

BALTEJ SINGH GILL
ROLL No. 601002001

Under the guidance
of
Dr. Puneet Sharma
Assistant Professor

(School of Physics and Materials Science)

School of Physics and Materials Science
Thapar University, Patiala
Patiala (Punjab)-147004

June-2012

CERTIFICATE

This is to certify that the thesis entitled **"Effect of particle size on the Magnetic properties of Barium hexaferrite bonded magnets"** *submitted by* **Mr. Baltej Singh Gill,** *Roll No.* **601002001** *in the partial fulfillment of the requirement for award of the degree of* **Mater of Technology** *in Materials and Metallurgical Engineering from the School of Physics and Materials Science,* **Thapar University, Patiala,** *is record of candidate's own work carried out by him under my supervision and guidance. The matter embodied in this report has not been submitted in part or full to any other university or institute for the award of any degree.*

Dr. Puneet Sharma

(Assistant Professor)

School of Physics and Materials Science

Thapar University

Patiala, Punjab

Countersigned By:

Dr. Kulvir Singh

(Associate Professor and Head)

School of Physics and Materials Science

Thapar University

Patiala, Punjab

Dr. S.K. Mohapatra

Dean, Academic Affairs

Thapar University

Patiala, Punjab

ACKNOWLEDGEMENT

First of all I would like to extend my gratitude towards my supervisor, **Dr. Puneet Sharma** (Assistant Professor), School of Physics and Materials Science, Thapar University, Patiala, for giving me a chance to work in his supervision and without his help and constant guidance this thesis would have not completed.

I wish my sincere thanks to **Dr. Kulvir Singh** (Associate Professor and Head), School of Physics and Materials Science, who always took keen interest in guiding me during my work.

I would also like to thank **Dr. O.P. Pandey,** Sr. Professor, and **Dr. Bhupendrakumar Chudasama**, Assistant Professor, School of Physics and Materials Science for their constant guidance and encouragement. I am grateful to them for sharing their time and expertise.

I am also grateful to **Mrs. Samiksha Verma**, Research Scholar, School of Physics and Materials Science for her encouragement and execution of report work and providing me invaluable support and training in various techniques and uses of equipment.

My special thanks to P.G. Lab Incharge **Mr. Purushottam** and **Mr. Jant Singh**, for their all kind of help in PG Lab for creating a healthy research environment.

I would also like to thank **Mr. Jagtar Singh,** (Sophisticated Analysis and Instrument Centre, Panjab University, Chandigarh) for carrying out the X-ray diffraction needed for my work.

I would like to give my special thanks to Research Scholars Mintu Tyagi, Samita Thakur, Param jha and Chandni Bansal for helping me at various stages of my experimental work.

I would also like to thank all the staff members of School of Physics and Materials Science for their support and encouragement.

I would also like to thank my parents for their all kind of support, encouragement and blessings. I am also very thankful to all my friends for their motivation and huge support.

(Baltej Singh Gill)

Roll No. 601002001

Dedicated

To

My Parents

INDEX

Contents		Page no.
List of symbols and abbreviations		I
List of Figures		II
List of Tables		III
Abstract		IV
CHAPTER 1	**INTRODUCTION**	**1-15**
1.1 Magnetic materials		1
1.2 Soft magnetic materials		1
1.3 Hard magnetic materials		2
1.4 Classification of hard magnetic materials		3
1.4.1 AlNiCo – Magnets		4
1.4.2 Rare-earth magnets		5
1.5 Hard ferrites		6
1.6 M-type ferrites		7
1.7 Crystal structure, magnetic structure and phase diagram of M Type ferrites		7
1.8 Intrinsic magnetic properties of M-type ferrites		11
1.9 Processing methods of hard ferrites		12
1.9.1 Solid state synthesis method		12
1.9.2 Chemical Co-precipitation methods		12
1.9.3 High energy ball milling method		13

1.9.4 Sol-gel method 14

1.10 Application of hard ferrites 14

CHAPTER 2 LITERATURE REVIEW 16-21

CHAPTER 3 EXPERIMENTAL DETAILS 22-24

3.1 Preparation of barium hexaferrite 22

CHAPTER 4 RESULTS AND DISCUSSION 25-35

4.1 XRD analysis 25

4.2 Particle Size measurements 28

4.3 SEM analysis 30

4.4 Magnetic measurements 32

CONCLUSION 36

REFERENCES 37-39

List of Symbols and Abbreviations

H_c	Coercivity
B_r	Remanance
B	Magnetic flux density
H	Magnetizing force
T_c	Curie temperature
M_s	Saturation magnetization
K_1	Anisotropy constant
XRD	X-ray diffraction
SEM	Scanning electron microscope
DTA	Differential thermal analysis
VSM	Vibrating sample magnetometer

List of Figures

Figure 1.1	Hysteresis loop for soft magnetic materials
Figure 1.2	Hysteresis loop for hard magnetic materials
Figure 1.3	Structure of barium hexaferrite
Figure 1.4	Phase diagram of Fe_2O_3-BaO system
Figure 3.1	Flow chart of making barium hexaferrite
Figure 3.2	Flow chart of making bonded magnet
Figure 4.1	X-ray diffraction pattern of Barium hexaferrite ($BaFe_{12}O_{19}$) at different milling hours (a) 1 hour milling (b) 2 hours milling (c) 3 hours milling (4) 4 hours milling
Figure 4.2	Variation in crystallite size of barium hexaferrite with milling time
Figure 4.3	Weight percentage of barium hexaferrite after (a) 1 h (b) 2 h (c) 3 h (d) 4 h ball milling
Figure 4.4	SEM micrographs of Barium hexaferrite powder (a) 1 h (b) 3h milling
Figure 4.5	Particle size percentage of barium hexaferrite powder after 1 hour and 3 hours milling calculated from SEM micrographs
Figure 4.6	M-H behavior of barium hexaferrite milled after (a) 1 h (b) 2 h (c) 3h (d) 4h
Figure 4.7	Variation in coericivity at different milling hours

List of Tables

Table 1.1	Comparison of commercial permanent magnetic materials
Table 1.2	Types of ferrites and their respective chemical formulae
Table 1.3	Crystallographic properties of M-type ferrite
Table 1.4	Primary and secondary properties of M-Type ferrites
Table 4.1	Crystallite size and lattice parameter of barium hexaferrite
Table 4.2	The comparative weight fractions of powders subjected to different milling time.
Table 4.3	Coericivity , saturation magnetization and M_r at different milling hours

ABSTRACT

In the present work barium ferrite compression bonded magnet with different particle size were prepared. To start this barium hexaferrite powder was prepared by solid state synthesis method. The calcined powder milled for different time to obtain the powder of different size. The chosen ball milling times were 1 h, 2 h, 3 h and 4 h. The particle size distribution was studied by mechanical sieving of powder. The prepared powders were mixed with epoxy resin and pressed in cylindrical die using hydraulic press. Phase and microstructural characterization was carried out by X-ray diffractometer and scanning electron microscope. XRD pattern shows the single phase barium hexaferrite. It is found that with increasing milling time the crystallite size decreases. From the SEM images it is found that the average particle size of powder decreases from 0.7μm to 0.5μm as the milling time increases. The magnetic properties were measured by vibration sample magnetometer. The result shows as the milling time increases the coercivity increases. The saturation magnetization remains same for all the bonded magnets.

Chapter 1

Introduction

1.1 Magnetic materials

Magnetic materials are those materials that can be either attracted or repelled when placed in external magnetic field and can be magnetized themselves. Common examples of magnetic materials are iron and its alloys which are used in various electrical appliances to increase the magnetic flux without increasing the current [1].

Magnetic materials can be divided into two groups:-

1. Soft magnetic materials: - The soft magnetic materials are those materials which are magnetized and demagnetized easily.

2. Hard magnetic materials: - The hard magnetic materials are those which are difficult to magnetize and demagnetize.

1.2 Soft magnetic materials

Soft magnetic materials can be easily magnetized and demagnetized. They retain their magnetization only in presence of a magnetic field. They show a narrow hysteresis loop, so that the magnetization follows the variation of applied field nearly without hysteresis loss [2]. They are used to enhance the flux, produced by an electric current in them. The quality factor of a soft magnetic material is to measure its permeability with respect to the applied magnetic field. The other main parameter is the coericivity, saturation magnetization and the electrical conductivity. An ideal soft magnetic material would have low coericivity (H_c), a very large saturation magnetization (M_s), zero remanance (B_r), zero hysteresis loss and very large permeability [3]. Few important soft magnetic materials are Fe, Fe-Si alloys, soft ferrites ($MnZnFe_2O_4$), silicon iron etc.

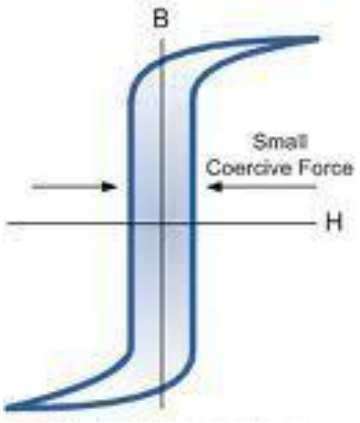

Figure 1.1: Hysteresis loop for soft magnetic materials

1.3 Hard magnetic materials

Hard Magnetic materials also called as permanent magnets are used to produce strong field without applying a current to coil. Permanent magnets required high coercivity, so they should exhibit a strong net magnetization and is stable in the presence of external fields. Hard magnetic materials have large uniaxial magnetic anisotropy. The magnetic properties of hard magnetic materials are explained below [4].

1. High coercivity: The coercivity of a ferromagnetic material is the intensity of the applied magnetic field required to reduce the magnetization of that material to zero after the magnetization of the sample has been driven to saturation. Coercivity is usually measured in oersted or ampere/meter units and is denoted H_c. Materials with high coercivity are called hard ferromagnetic materials, and are used to make permanent magnets [5].
2. Large magnetization: The process of making a substance temporarily or permanently magnetic, as by insertion the material in a magnetic field.
3. Rectangular hysteresis loop: A hysteresis loop shows the relationship between the induced magnetic flux density (B) and the magnetizing force (H). Hard magnetic materials have rectangular hysteresis loop [6]

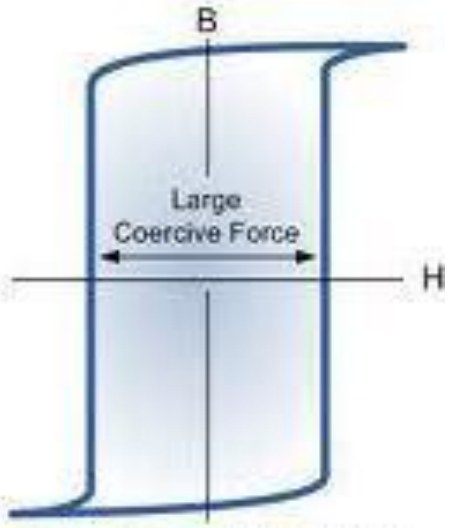

Figure 1.2: Hystersis loop for hard magnetic materials

1.4 Classification of hard magnetic materials

Among the permanent magnetic materials the important materials are alnico, hard ferrite, samarium cobalt and neodymium-iron-boron. Each of these materials exhibits different set of properties. By comparison with production cost, the hard ferrites found to be the most suitable. A comparison of commercial permanent magnets is given in Table 1.1. By comparing the cost of different materials it is found that ferrites are most economical and also the rare earth based magnets have better magnetic properties as compared to ferrite [7].

Table 1.1 : Comparison of commercial permanent magnetic materials

Parameter	**AlNiCo**	**$SmCo_5$**	**Nd-Fe-B**	**Ferrite**
B_r (mT)	700-1200	890	1100	370
H_{ci} (kA/m)	50-150	1200	>1000	255
$(BH)_{max}(kJ/m^3)$	60-80	150	350	30
$T_c(K)$	860	933	585	750
Max. Operation Temperature(K)	773	523	373	523
Raw material source	Poor	Poor	Good	Very good
Density(kg/m^3)	7300	8300	7400	4650
Price ratio/ Magnetic energy	7.5	23	7	1

1.4.1 AlNiCo – Magnets

Raw materials for AlNiCo magnets are aluminium nickel, cobalt, iron and titanium. AlNiCos are produced in a sintering - casting procedure. The hard material needs to be processed by grinding to be cost effective. Due to its specifications, the best dimension is a remarkably longer length than its diameter. In combination with reed sensors / switches we recommend a length / diameter ratio of more than 4. AlNiCo magnets have excellent temperature stability. Negative point is the high raw material prices [8].

Main features of AlNiCo:-

1. Working temperature from -250 to 450^oC.
2. Low temperature coefficient.

1.4.2 Rare - earth magnets

Rare - Earth magnets like $SmCo_5$ and NdFeB have the highest energy density per volume and weight and also the best demagnetizations resistance. Both magnets are produced by sintering and can only be processed by grinding, due to the strength and brittle of the material. Disadvantages of the rare earth magnets are high raw material prices and the limited availability of special alloys. The supply of different geometry, size and magnetization allow many creative combinations of reed sensor / switch and magnet and help to find the best functionality of the sensor magnet system for each application [8].

Main features of $SmCo_5$:-

1. High energy density.
2. Small size.
3. Best opposing field resistance.
4. Available plastic bounded.

Main features of NdFeB:-

1. High energy density.
2. Small size.
3. Lower price compare to SmCo.
4. Available plastic bounded.

Among the class of hard magnetic materials the hard ferrite are very important due to its moderate magnetic properties at lower cost.

1.5 Hard ferrites

The term ferrite is commonly used generically to describe a class of magnetic oxide compounds, which contains iron oxide as a principal component. Magnetite, Fe_3O_4 also called loadstone, is a genuine ferrite and also was the first magnetic materials known to the ancient people. Ferrites can be classified according to crystal structure, i.e. cubic vs. hexagonal ferrite, or magnetic behavior, i.e. soft vs. hard ferrite. Hard ferrite magnets are produced with iron oxide and barium or strontium oxide. The raw materials are mixed together and normally pre sintered, to generate the magnetic phase. The pre sintered mixture then gets crushed. The resulting powder gets pressed together (wet or dry) either in a magnetic field (an - isotropic) or without a magnetic field (isotropic) and in the end sintered. Proceedings are only possible by grinding. Due to the low cost of the raw material, hard ferrite magnets are the cheapest magnet type out of the actual supply of magnets. Ferrites have a very good electrical isolation effect and are hard to demagnetize even in strong external magnetic fields. Corrosion tendency is low. Preferred shapes are long and thin but also round forms are easy to produce. Disadvantages are the high breakability and the low tensile strength. The strength and brittleness of hard ferrites are similar to ceramics. Hard ferrites have a hexagonal structure and can be classified as M-, W-, X-, Y-, Z-, U- type ferrites [9].

Main features of hard ferrites: -

1. Cheapest magnetic material.
2. Many options in form and magnetization.
3. Available plastic bounded.

Table 1.2 Types of ferrites and their respective chemical formulae.

Types	Chemical formula	
M-	$RFe_{12}O_{19}$	R = Ba, Sr, Pb
W-	$RMe_2Fe_{16}O_{27}$	Me = Fe^{+2}, Ni^{+2}, Mn^{+2} etc
X-	$R_2Me_2\ Fe_{28}O_{46}$	
Y-	$R_2Me_2Fe_{12}O_{22}$	
Z-	$R_3Me_2Fe_{24}O_{41}$	
U-	$R_4Me_2Fe_{36}O_{60}$	

1.6 M-type ferrites

M-type ferrites with the formulae of $BaO.6Fe_2O_3$ (BaM), $SrO.6Fe_2O_3$ (SrM) and $PbO.6Fe_2O_3$ (PbM) are by far the most important hexagonal ferrites. M-type ferrites are mainly used as permanent magnet materials that have strong resistance to demagnetizing field once they get magnetized and have a dominant position in permanent magnet market. They are preferred over alnicos due to lower material and processing cost and superior coercivity. Sr-Ferrite and Ba-Ferrite are the two main materials in the M-type ferrite family. These ferrites have moderate magnetic properties, and price per unit of available magnetic energy is very less.

1.7 Crystal structure, magnetic structure and phase diagram of M Type ferrites

The crystalline and magnetic structures of the different types of hexaferrites are remarkably complex, as shown for the most important M-hexaferrite $BaFe_{12}O_{19}$ in Figure 1.3. The elementary unit cell contains ten oxygen layers, sequentially constructed for four blocks: S (spinel), R (hexagonal), S* and R*. The S* and R* blocks have equivalent atomic arrangements, but rotated at 180^o with respect to S and R blocks around the c-axis. An S or S* block consists of two O^{2-} layers; while R or R* block contains three O^{2-} layers, with one

oxygen site in the middle layer substituted by an Ba^{2+} ion [10]. Hexagonal ferrites of the M-type are still of enormous technical importance in the permanent magnet market because of their low price combined with reasonable magnetic performances. For this reason, a little improvement of their magnetic or dielectric properties is of great relevance. The M-type ferrite ($SrFe_{12}O_{19}$) crystallizes in a hexagonal structure with 64 ions per unit cell on 11 sites of different symmetry. 24 Fe^{3+} atoms are distributed over five distinct sites: three octahedral sites (12k, 2a and 4f2), one tetrahedral site (4f1) and one bipyramidal site (2b). The magnetic structure given by the Gorter model is ferrimagnetic with five different sub lattices, three parallel (4f1 and 4f2) which are coupled by super exchange interactions through the O^{2-} ions. A significant improvement of the intrinsic magnetic properties of M-type ferrites can be obtained by the partial substitution of Sr^{2+} , Ba^{2+} or Fe^{3+} ions, or both [11,12].

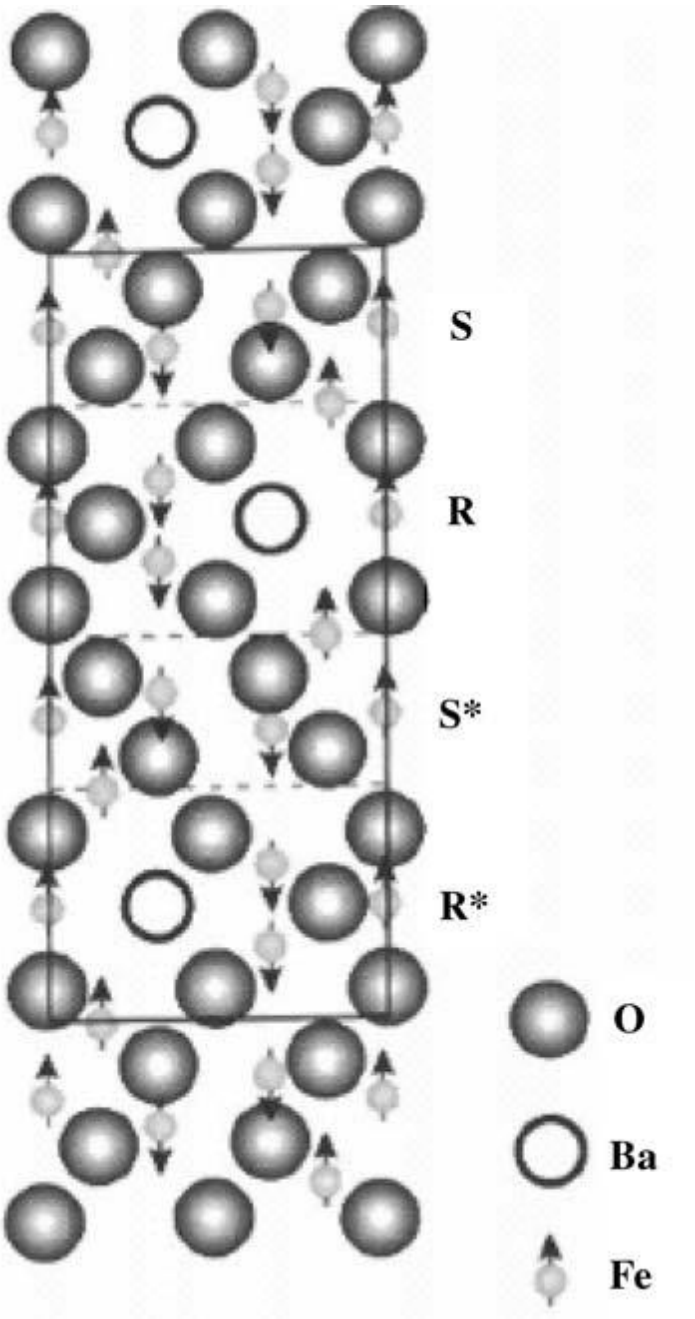

Figure 1.3: Structure of barium hexaferrite

Table 1.3: Crystallographic properties of M-type ferrite.

Parameter		Ferrite(s)		
Lattice Constant (nm)	a	BaM	SrM	PbM
		0.5893	0.588	0.588
	c	2.3194	2.307	2.302
Molecular wt.		1112	1062	1181
Density gm/cc		5.28	5.11	5.68

Figure 1.4 shown below shows the phase diagram of BaO and Fe_2O_3 system. In the phase diagram the homogeneity range is very narrow and in the eutectic range somewhat enlarged, at most towards the side rich in the BaO [13].

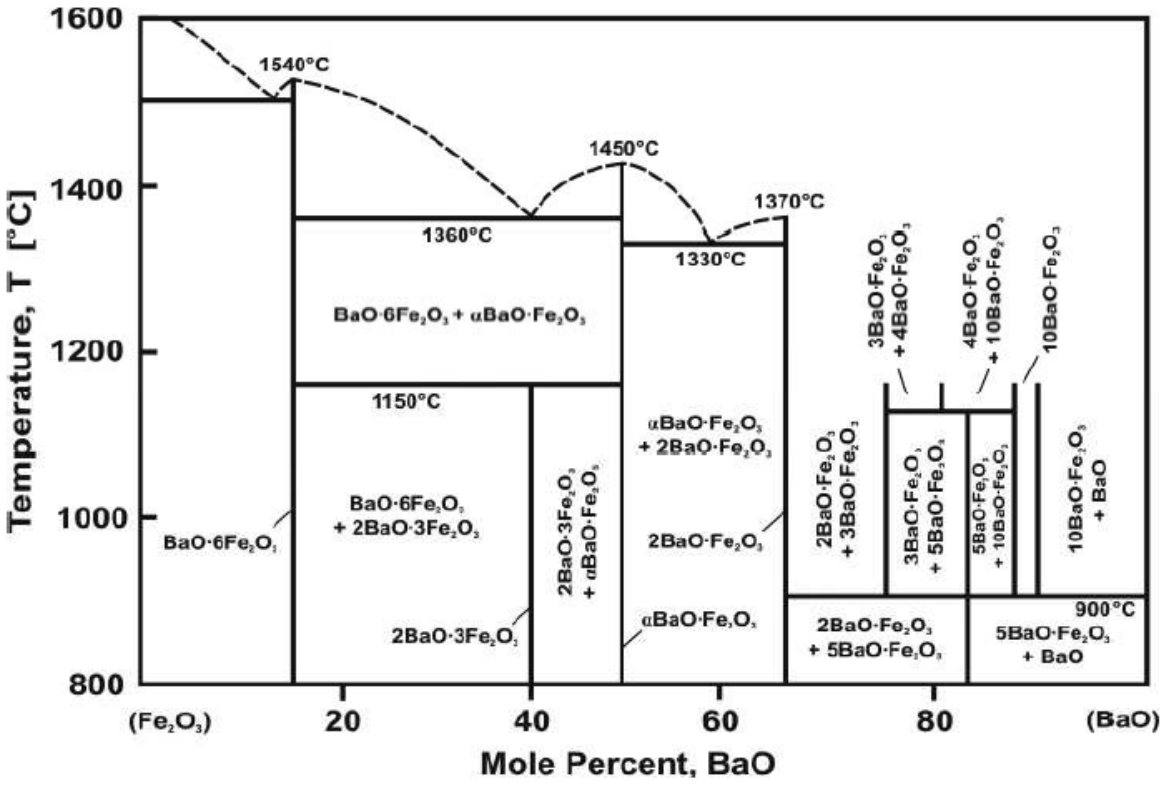

Figure 1.4: Phase diagram of Fe_2O_3-BaO system.

Towards higher temperature range, incongruent melting occurs at 1448 ^{0}C (1 bar O_2) and 1390^{0}C (air), with the W phase $BaFe_{18}O_{27}$ (= BaO 2FeO.8Fe_2O_3) is formed [14]. However, in vacuum annealing above 1100 ^{0}C, Fe_3O_4 and S7F5 phase is formed with the release of oxygen, where S= 2(BaO.Fe_2O_3) and F= BaO. 6Fe_2O_3 or $BaFe_{12}O_{19}$ phase is stable only towards lower temperature range. Towards the Fe_2O_3 richer side the two phase region ($BaFe_{12}O_{19}$ + Fe_2O_3) are formed. On the BaO richer region, the phase S7F5 and S3F2 are the neighbouring phases both of them being very close to the composition S4F3 [15]. The eutectic temperatures of 1210 ^{0}C (1 bar O_2) or 1195 ^{0}C (air) as well as the eutectic content of 53.5 or 55 mole % are close to one another.

1.8 Intrinsic magnetic properties of M-type ferrites

The intrinsic magnetic properties are subdivided into primary and secondary one. The primary properties such as saturation magnetization J_s and magneto crystalline anisotropy constant K_1 are directly related to the magnetic structure. The secondary magnetic properties such as anisotropy field strength H_A and the specific domain wall energy (γ_w) are derived from the primary ones. The secondary magnetic properties characterize the actual magnetic state. These govern the actual magnetic behavior. The primary and secondary magnetic properties characterize the actual magnetic state. These govern the actual magnetic behavior. The primary and secondary magnetic properties are shown in table 1.4.

Table 1.4: Primary and secondary properties of M-Type ferrites.

Primary Properties	
Saturation Magnetization, mT	475
Anisotropic constant, kJ/m^3	360
Curie temperature, K	750
Secondary Properties	
Specific wall energy, J/m^2	54.2 x 10^{-4}
Anisotropy Field H_A, kA/m	1506
Max Coercivity, $(H_c)_{max}$	1240

1.9 Processing methods of hard ferrites

There are various types of methods to process hard ferrites which can classify in major four types:

1. Solid state synthesis method
2. Chemical Co-precipitation methods
3. High energy ball milling method
4. Sol-gel method

1.9.1 Solid state synthesis method

Among the various processing method solid state synthesis is widely used. The solid state synthesis is basically a diffusion method. This method starts with mixing of barium carbonate and iron chloride to homogenize the raw materials, and can take place either with a wet or dry process. In wet mixing, generally using an aqueous suspension, vibration drum or agitator mills are used. Dry mixing is done either by grinding and mixing in drum or ball mills or intensive mixing in an edge runner mill or in high intensity counter flow mixer with swirler. The first method is used when the raw materials are not fine enough for the subsequent reaction. Using second method, the materials can be fed directly to the reaction furnace. Calcination facilitates solid state diffusion of BaO and Fe_2O_3 and converts the raw materials into the hexaferrite phase. The calcination temperature also plays an important role in the formation of hexaferrite phase. If the calcination temperature is low, then grains of uniform BaM are not formed. Similarly, if the calcination temperature is too high, excessive grain growth occurs and coarse grain BaM is formed [17].

1.9.2 Chemical Co-precipitation methods

Co-precipitation (CPT) is carrying down by a precipitate of substances normally soluble under the conditions employed. In medicine, co-precipitation is specifically the precipitation of an unbound "antigen along with an antigen-antibody complex". There are three main mechanisms of co-precipitation: inclusion, occlusion, and adsorption [18]. An inclusion occurs when the impurity occupies a lattice site in the crystal structure of the carrier, resulting in a crystallographic defect, this can happen when the ionic radius and charge of the

impurity are similar to those of the carrier. An adsorbate is an impurity that is weakly bound (adsorbed) to the surface of the precipitate. An occlusion occurs when an adsorbed impurity gets physically trapped inside the crystal as it grows [19].

1.9.3 High energy ball milling method

Ball mill is a good tool for grinding many materials into fine powder. The Ball Mill is used to grind many kinds of mine and other materials. There are two type of grinding: the dry process and the wet process. It can be divided into tabular type and flowing type according to different forms of discharging material. After the grinding the state of the solid is changed: the size and shape of grain etc. Ball mill is horizontal type and tubular running device has two warehouses. This machine is grid type and its outside runs along gear. The material enters spirally and evenly the first warehouse of the milling machine along the input material hollow axis by input material device. In this warehouse, there is a ladder scale board or ripple scale board, and different specification steel balls are installed on the scale board, when the barrel body rotates and then produces centrifugal force , at this time , the steel ball is carried to some height and falls to make the material grinding and striking. After grinded coarsely in the first warehouse, the material then enters into the second warehouse for regrinding with the steel ball and scale board. In the end, the powder is discharged by output material board and the end products are completed. The ball mill is a key equipment for grinding. It is widely used for the cement, the silicate product, new type building material, fire-proof material, chemical fertilizer, black and non-ferrous metal, glass, ceramics and etc. Ball mill can grind ore or other materials that can be grinded either by wet process or by dry process [20].

Benefits of ball mill:-

- Increase of the surface area of a solid
- Manufacturing of a solid with a desired grain size
- Pulping of resources

1.9.4 Sol-gel method

In this method, the 'sol' gradually evolves towards the formation of a gel-like diphase system containing both a liquid phase and solid phase whose morphologies range 26 from discrete particles to continuous particles. In the case of the colloid, the volume fraction or density of particles may low that a significant amount of fluid may need to be removed initially for the gel-like properties to be recognized [21]. To removing of the remaining liquid phase apply a drying process. The rate at which the solvent can be removed is ultimately determined by the distribution of porosity in the gel. The microstructure of the final component will clearly be strongly influenced by changes imposed upon the structural template during this phase of processing. After this, a thermal treatment or firing process is necessary for further polycondensation. When we do the final sintering, we found enhance mechanical properties, structural stability, densification and grain growth [22]. The sol-gel technique is a cheap and low-temperature technique that allows for the fine control of the product's chemical composition. Sol-gel derived materials have diverse applications in optics, electronics, energy, space etc [23].

1.10 Application of hard ferrites

Hard ferrites are very important magnetic materials because of their high electric resistivity; they have wide applications in technology, particularly at high frequencies. Hard ferrites are used widely due to their following properties.

1. Ferrites are part of low power and high flux transformers which are used in television.
2. Small antennas are made by winding a coil on ferrite rod used in transistor radio receiver.
3. In computer, non volatile memories are made of ferrite materials. They store information even if power supply fails. Non-volatile memories are made up of ferrite materials as they are highly stable against severe shock and vibrations.
4. Hard ferrites are used in microwave devices like circulator, isolators, switches Phase Shifters and in radar circuits.

5. Hard ferrites are used in high frequency transformer core and computer memories i.e computer hard disk, floppy disks, credit cards, audio cassettes, video cassettes and recorder heads.
6. Hard ferrites used in magnetic tapes and disks are made of very small needle like particles of Fe_2O_3 or CrO_2 which are coated on polymeric disk. Each particle is a single domain of size 10-100 nm.
7. Iron-silicon alloys are used in electrical devices and magnetic cores of transformers operating at low power line frequencies. Silicon steel is extensively used in high frequency rotating machines and large alternators.
8. Nickel alloys are used in high frequency equipments like high speed relays, wide band transformers and inductors. They are used to manufacture transformers, inductors, small motors, synchros and relays. They are used for precision voltage and current transformers and inductive potentiometers.
9. They are used as electromagnetic wave absorbers at low dielectric values.
10. Ferro fluids, as cooling materials, in speakers. They cool the coils with vibrations.

Chapter 2

Literature review

Since the discovery of the M-type hexagonal ferrites in 1950s, it has being of great interest due to its application as permanent magnetic materials and perpendicular recording media. The main reason for its great success is its low cost at moderate magnetic properties. Various works has been carried to develop hexaferrite by various methods and their properties have been investigated. Work carried out in past few years on different processing methods and different dopants are given below:

In 2006 **Ali Ghasemi *et al.*** [24] analyzed structures, electromagnetic and microwave absorption properties of prepared ferrites with the help of X-ray diffraction (XRD), scanning electron microscope (SEM), vector network analyzer and a.c. susceptometer. Their results showed that the magnetoplumbite structures for all the samples have been formed. They demonstrated that Microwave absorbers for the applications over 15 GHz, and with satisfactory reflection losses, could be obtained at a matching thickness of 1.8 mm by controlling the substituted value of Mn^{2+} and Ti^{4+} elements in barium ferrite.

In 2009 **Tzu-Hao Ting *et al.*** [25] synthesized Polyaniline / $BaFe_{12}O_{19}$ (PANI / Ba) composite by in situ polymerization at different aniline / Ba weight ratios and introduced into epoxy resin to be microwave absorber. They studied the spectroscopic characterizations of PANI/ Ba composites using Fourier transform infrared, ultraviolet–visible spectro-photometer, X-ray diffraction, scanning electron microscopy, transmission electron microscopy and electron spin resonance. They investigated microwave-absorbing properties by measuring complex permittivity, complex permeability and reflection loss in the 2–18 and 18–40 GHz microwave frequency range using the free space method. Their results indicated that the composites exhibit good absorption performances over abroad- band range in the

radar band (2–40 GHz) with good electro- magnetic properties. The PANI/Ba powder showed better absorption bands than Ba ferrite at 2–18 GHz.

In 2006 **S.M. Abbas *et al.*** [26] investigated the complex permittivity (ε′–jε′′), complex permeability (μ′–jμ′′) and microwave absorption properties of ferrite–polymer composites prepared with different ferrite ratios of 50%, 60%, 70% and 80% in polyurethane (PU) matrix in X-band (8.2–12.4 GHz) frequency range. They prepared M-type hexaferrite composition $BaCo^{+2}_{0.9}\ Fe^{+2}_{0.05}Si^{+4}_{0.95}Fe^{+3}_{10.1}O_{19}$ by solid-state reaction technique, whereas commercial PU was used to prepare the composites. They found that all the parameters ε′, ε′′, μ′ and μ′′ with increased ferrite contents. The composite with 80% ferrite content has shown a minimum reflection loss of --24.5 dB (>99% power absorption) at 12GHz with the --20 dB bandwidth over the extended frequency range of 11–13GHz for an absorber thickness of 1.6 mm. The prepared composites can fruitfully be utilized for suppression of electromagnetic interference (EMI) and reduction of radar signatures (stealth technology).

In 2009 **S.P. Gairola *et al.*** [27] investigated the magnetic and electromagnetic wave absorbing properties of the Co-Mn-Ti substituted barium ferrites, $BaCo_xMn_xTi_{2x}Fe_{12-4x}O_4$ ($0 \leq x \geq 0.5$). The grain size uniformity and densification improved with increasing concentration of Co-Mn-Ti, while the permeability increased and the coercivity decreased remarkably. They measured the reflection coefficients (S_{11}, S_{12}) of the ferrite samples in the X-band frequency range (8-12 GHz) and calculated their absorbing properties according to transmission line theory. The maximum reflection loss (-14.7 dB) is observed for the x = 0.4 sample. A ferromagnetic resonance frequency shift has been observed to depend on the Co-Mn-Ti concentration, which is an important phenomenon of barium ferrite for absorbing microwaves at high frequencies. Based on the magnetic and microwave measurements, $BaCo_xMn_xTi_{2x}Fe_{12-4x}O_4$ may be a good potential candidate for electromagnetic compatibility and for other practical applications at high frequencies.

In 2002 **Zhang Haijun *et al.*** [28] prepared $Ba(ZnTi)_xFe_{12-2x}O_{19}$ (x varies from 0.2 to 1.0 in steps of 0.2) hexaferrites by citrate sol- gel process, the formation temperature is about 800 °C . They characterized the samples by XRD, scanning electron microscopy. They studied

the effect of $Zn^{2+}Ti^{4+}$ substitution, annealing temperature on complex permeability, permittivity and microwave absorption for $Ba(ZnTi)_xFe_{12-2x}O_{19}$ ferrite in the frequency range from 100 MHz to 6.0 GHz. All the ferrites exhibit significant dispersion in complex permeability. The dispersion in complex dielectric constant is not significant. The variations of reflection loss have been studied as a function of frequency, $Zn^{2+}Ti^{4+}$ content, and thickness of the absorber. Their results show that BaM ferrite can be prepared at about 800 °C. The calculation results of transmission line theory show that the reflection loss value is small for $Ba(ZnTi)_x$ - $Fe_{12-2x}O_{19}$ ferrites in 100 MHz - 6.0 GHz.

In 2006 **P. Sharma *et al.*** [29] prepared barium hexaferrite powders by ordinarily mixing and by high energy ball-milling stoichiometric amounts of the $BaCO_3$ and Fe_2O_3 precursors, followed by heat treatments carried out in the 900–1100 °C range of temperature. They analyzed the structural and magnetic properties of the resulting powders by differential thermal analysis, X-ray diffraction, scanning electron microscopy, Mössbauer spectroscopy and magnetization measurements. They observed the formation of $BaFe_2O_4$ intermediate phase in conventionally prepared hexaferrites. The results showed that 30 h of milling increases the specific surface area more than three times over the un-milled powders and reduces the temperature for hexaferrite phase formation to 900 °C. However, the hyperfine properties were shown to be independent from the processing methods. The H_C enhancement in the mechanically alloyed samples were attributed to its smaller particle size as compared to the conventionally prepared samples and were not due to a refined crystallite size as usually pointed out.

In 2010 **Mohsen Q *et al.*** [30] studied the effect of different annealing temperature on the particle size, microstructure and magnetic properties of the resulting barium hexaferrite powders. The annealing temperature was in the range 800 to 1200 °C. They investigated resultant powders by differential thermal analyzer (DTA), X-ray diffractometer (XRD), scanning electron microscopy (SEM) and vibrating sample magnetometer (VSM). Single phase of $BaFe_{12}O_{19}$ was obtained at annealing temperature 1200 °C. The SEM results showed that the grains were regular hexagonal platelets. Maximum saturation magnetization

(66.36 emu/g) was observed at annealing temperature 1100 °C. However, it was found that the coercivity of the synthesized $BaFe_{12}O_{19}$ samples was lower than the theoretical values.

In 2001 **V. Babu *et al.*** [31] prepared barium hexaferrite by ball milling of a BaO_2 and Fe_2O_3 mixture followed by thermal heat treatments. They investigate structure and magnetic properties using X-ray diffraction, scanning electron microscopy and vibrating sample magnetometer techniques. They studied the effect of grain refiner and found that the hard magnetic properties improved significantly. They found that the sintered product of barium hexaferrite powders prepared from ball milling has higher coercive force than that of other barium hexaferrite made from oxide/carbonate.

In 2008 **P. Sharma *et al.*** [32] studied the Structural, Mössbauer and magnetic studies on Mn-substituted barium hexaferrites prepared by high energy ball milling and thermal annealing. The magnetization decreases with increasing the substitution amount due to the dilution of the magnetic structure. The increase in coercivity is due to the decrease in lattice parameter, c, which may enhance the super exchange interaction between neighboring ions.

In 2009 **Huseyin Sozeri *et al.*** [33] synthesized Barium hexaferrite three different routes, namely oxidation in nitric acid, solid state reaction and co-precipitation. It was shown that pelletizing before the sintering favors the formation of $BaFe_{12}O_{19}$ phase when metallic oxides are used as starting materials by increasing the reaction rates of the precursors. They observed the improvement in the saturation magnetization whereas the coercive field remained nearly the same with and without pelletizing in these samples. They investigated magnetic interactions using the Stoner–Wohlfarth model which showed that demagnetizing-like interactions become stronger in the pelletized samples prepared by oxidation in nitric acid and solid state reaction routes However; this interaction was suppressed in the pelletized sample prepared using co-precipitation technique by reducing the fraction of antiferromagnetic $Ba_2Fe_6O_{11}$ phase.

In 2001 **Silvia E. Jacobo *et al.*** [34] presented and discussed the evolution of macroscopic magnetic properties of $BaFe_{12}O_{19}$ synthesized by a new chemical coprecipitation method.

They investigated structural and magnetic properties by X-ray diffraction, scanning electronic microscopy and magnetic measurements on fine particles resulting from annealing treatments. High values of coercive field (4.4 kOe) and of the magnetization (70 emu g^{-1}) were obtained on well-crystallized $BaFe_{12}O_{19}$ particles annealed at 800°C.

In 1974 **Koichi Haneda *et al.*** [35] studied magnetic properties of $BaFe_{12}O_{19}$ prepared by chemical coprecipitation. They obtained a coercive force of 6000 Oe for isotropic $BaFe_{12}O_{19}$. X-ray and Moessbauer studies were conducted to examine the mechanism of formation. Superparamagnetic α-Fe_2O_3 was present during synthesis. They sintered the ferrites from these precipitated powders by both the usual method and a hot-press-forging method. The observed magnetic characteristics result from partial orientation of defect-free single-domain coprecipitated powders.

In 2006 **J.M. Soares *et al.*** [36] synthesized $BaFe_{12}O_{19}$ samples by an ionic-coordination-reaction (ICR) technique using chitosan as a complex agent. They controlled the mean size D_m of the particles and their magnetic properties by varying the concentration of chitosan in the starting solution. It was found that D_m, the coercive field H_C, and the Curie temperature T_C decrease when the concentration of chitosan is increased. Moreover, the variation in the magnetic parameter with D_m agrees well with those expected for a system of randomly distributed single-domain particles having positive uniaxial anisotropy, as proposed by current theoretical models.

In the 2010 **I. Bsoul *et al.*** [37] successfully investigate the Magnetic and structural properties of barium hexaferrite with its stoichiometric chemical formula $BaFe_{12}O_{19}$. In the present work concerned with the magnetic properties of BaM doped with gallium. In this study they suggest that the preferential site occupation of Ga below this particular concentration is different than at higher concentration. The effect of Ga substitution for Fe results in an increase in the coercivity, which is attributed to the decrease of the magnetic exchange coupling. The reduction in exchange coupling is confirmed by the broadening of SFD and the decrease in remanence ratio and Curie temperature with increasing Ga concentration.

In 2000 **N.W.K.** ***et al.*** [38] prepared fine particles of barium ferrite with high coercivity (450kA/m) by chemical co-precipitation method. Magnetic properties of the bonded barium ferrite magnet were measured at different temperatures. Mechanical milling was utilized to prepare ultrafine dispersed barium ferrite particles. A weak anisotropy in the coercivity and remanence was found in the directions parallel and perpendicular to the compaction direction.

Chapter 3

Experimental detail

.

3.1 Preparation of barium hexaferrite

The raw materials used in study were $BaCO_3$ and Fe_2O_3 (purity 99.0% Loba Chemicals). The composition of the sample was taken according to reaction equation given below:

$$BaCO_3 + 6Fe_2O_3 \rightarrow BaFe_{12}O_{19} + CO_2$$

The required composition of $BaCO_3$ and Fe_2O_3 was weighed according to above formula. Further both the materials were wet mixed for three hours in a planetary ball mill. Zirconia jar and ball were used for the mixing. The ball to charge ratio was 2:1 and rpm of the milling was fixed to 147. After milling, the excess acetone was drained and powder was dried in air. Further the powder were kept in alumina boat and calcined at 1200°C for 3 hrs. The heating cooling rate was fixed to 5 °C/minute and the holding time was 3 hours.

After that the resulting material was divided into four equal parts with help of weighing machine. Then the each part was wet milled for 1hour, 2 hours, 3 hours and 4 hours respectively using tungsten carbide jar and balls. The ball to charge ratio was fixed to 10:1 and rpm of milling was 176. After the milling the powder were dried.

Particle size distributions of the milled powder were carried out using sieve shaker and scanning electron microscopy model JEOL 6510. For SEM micrograph, the powders were placed on a copper mount and coated with thin layer of Au-Pd to make it conducting. The micrographs were taken in secondary electron mode.

To prepare the bonded magnets with different particle size, the powder milled for different duration were mixed with 5 % of epoxy resin and compressed in cylindrical die of diameter 1 cm using hydraulic press. The pressure was 10 ton/cm^2. The powder remained under

pressure for two hour to cure the binder. The magnetic measurement was carried out using vibration sample magnetometer (VSM). The maximum field of 1 T was applied with the step size of 200 Oe.

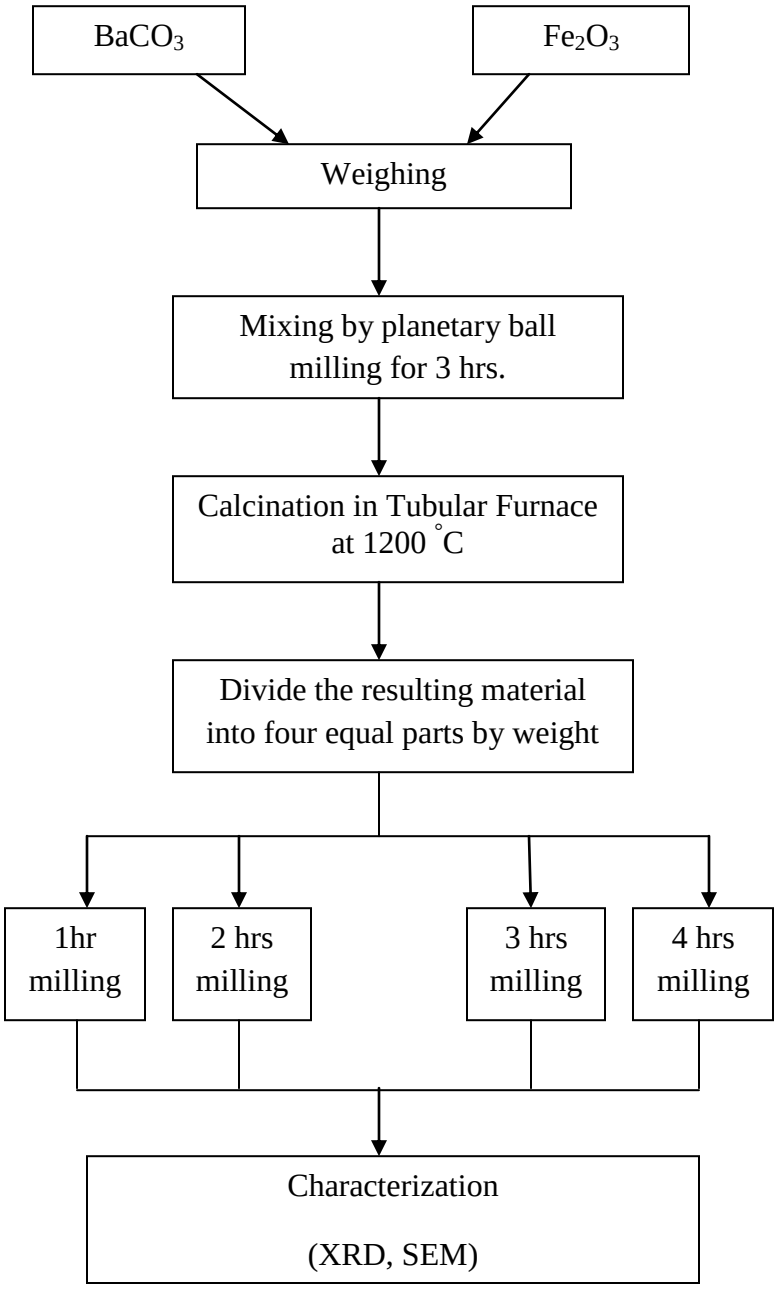

Figure 3.1: Flow chart of making barium hexaferrite

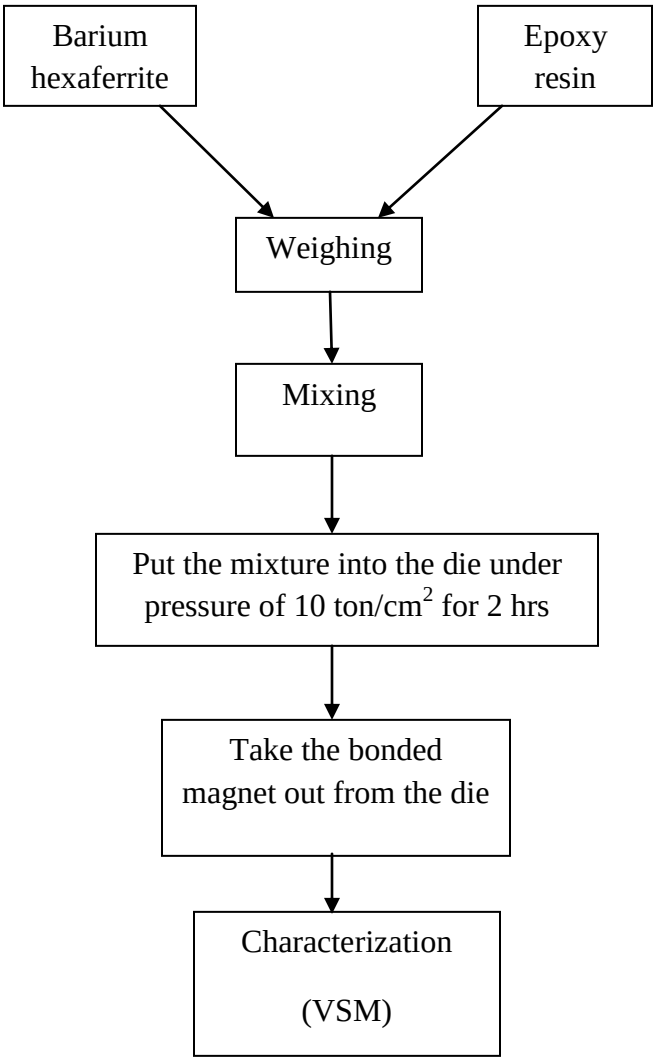

Figure 3.2: Flow chart of making bonded magnet

Chapter 4

Results and discussion

4.1 XRD analysis

Figure 4.1(a-d) shows the X-ray diffraction pattern of calcined Barium hexaferrite ($BaFe_{12}O_{19}$) powder at 1200^0C milled for 1 , 2 , 3 and 4 hours respectively. The XRD patterns were matched with JCPDS card no. 43-0002. All X-ray patterns show the single phase barium hexaferrite without any impurity and residual phase.

The crystallite size of barium hexaferrite is calculated by Debye Scherer formula.

$$D = \frac{k\lambda}{\beta \cos\theta}$$

where, D is the crystallite size, k is the Scherer constant, λ is the wave length of radiation (λ=1.54Å), β is the peak width at half maximum measured in radian, and θ the peak angle.

The lattice parameters are calculated with the formula:

$$\frac{1}{d^2} = \frac{4}{3}\frac{(h^2 + hk + k^2)}{a^2} + \frac{l^2}{c^2}$$

Where d is interplanar spacing, h, k and l are miller indices of the plane and 'a' and 'c' are lattice parameters.

Calculated crystallite size and lattice parameters (a and c) for barium hexaferrite are given in table 4.1. The variation of crystallite size is shown in fig. 4.2. It can be seen from the figure that crystallite has decreased from 137 nm to 118 nm, followed by a little increase in it. The little increase is may be attributed to recrystallization due to higher milling time. The lattice parameter calculated for all the powder are remain constant (table 4.1), since milling time only reduces the particle size not the unit cell. The lattice parameters can be varied by doping at Ba or Fe site. In the present case we prepared the pure Ba hexaferrite powders with no doping [39].

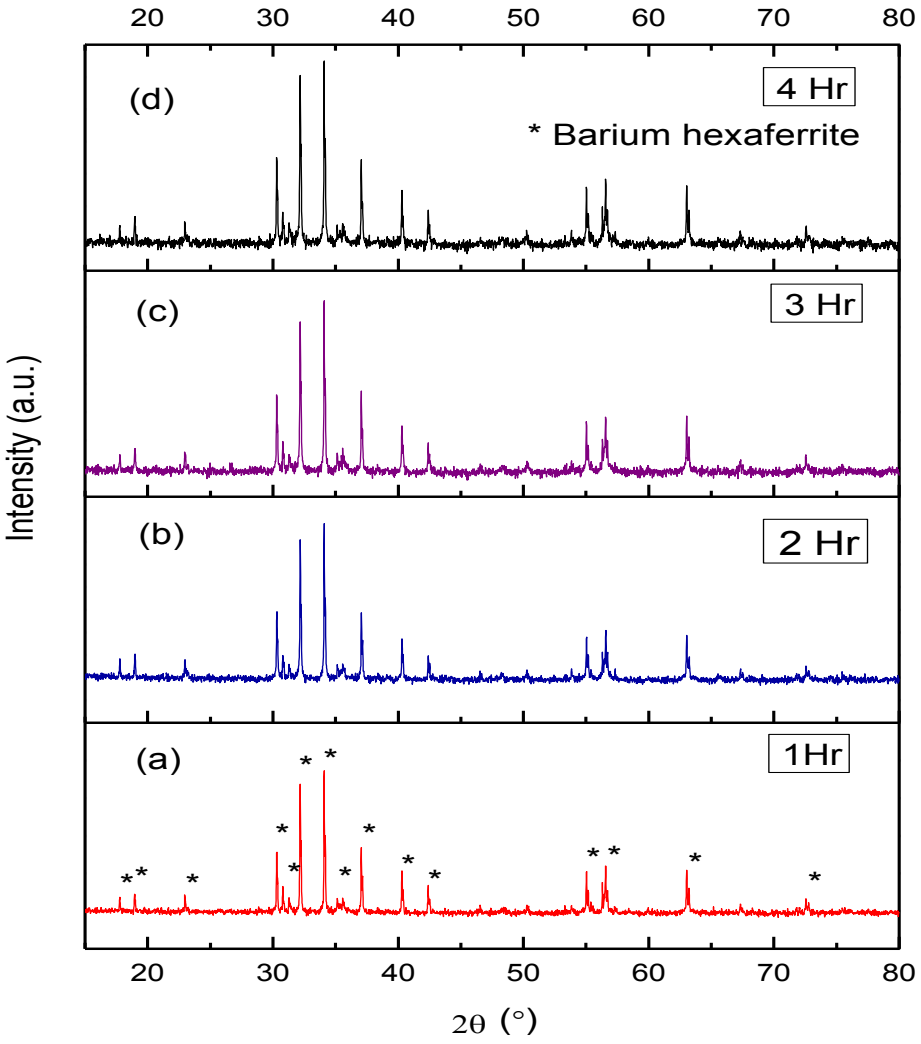

Figure 4.1: X-ray diffraction pattern of Barium hexaferrite ($BaFe_{12}O_{19}$) at different milling time. (a) 1 hour milling (b) 2 hours milling (c) 3 hours milling (4) 4 hours milling

Table 4.1: Crystallite size and lattice parameter of barium hexaferrite

Milling time (in hours)	a(Å)	c(Å)	Crystallite size(nm)
1	5.89	23.26	137.38
2	5.89	23.25	118.4
3	5.88	23.26	127.5
4	5.89	23.26	124.6

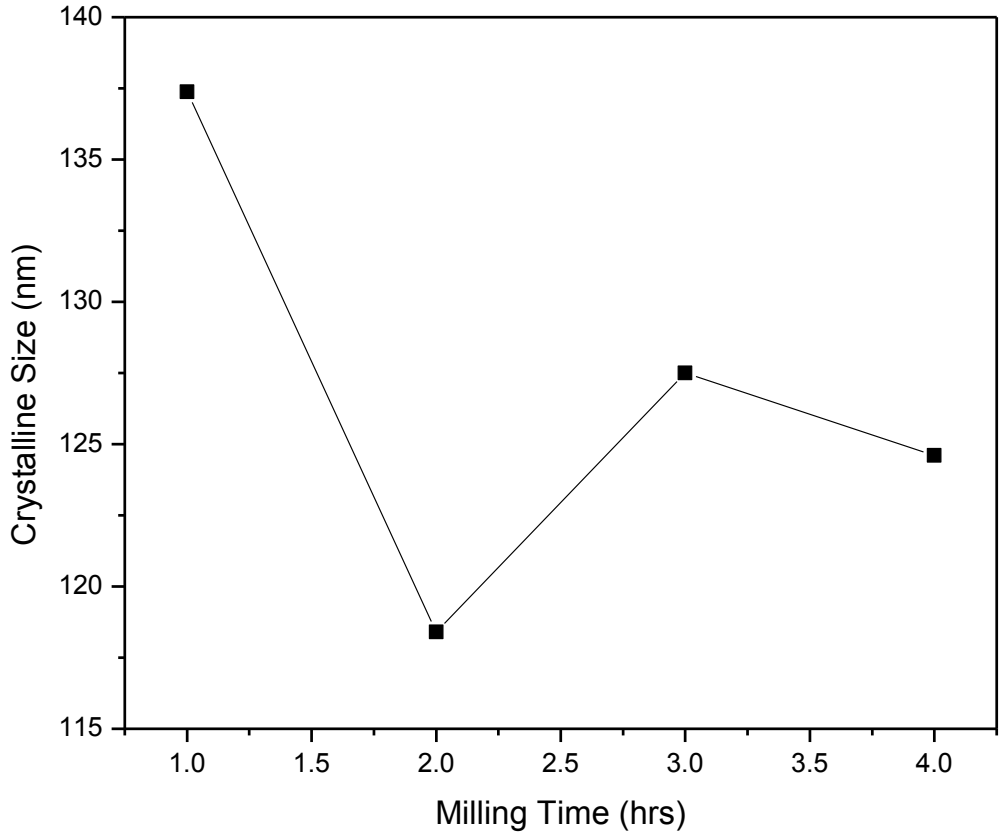

Figure 4.2: Variation in crystallite size of barium hexaferrite with milling time

4.2 Particle Size measurements

To find out the weight percentage of the particles in different size range, the powder was subjected to mechanical sieving using a sieve shaker. The sieves of 90, 75, 45 and 25 micron sizes were stacked and powder was put into the sieve of large size (90 micron). The stacked was vibrated for 10 minutes, the powder remained in all the sieves were collected and weighed.

Figure 4.3(a-d) shows the weight percentage of barium hexaferrite powder milled for different hours. It can be seen that after one hour milling the powder above 90 micron has near about 31% of total weight and then it decreases to 14% in 75 micron sieve. The sieve of 45 micron contains near about 33% weight and then it decreases to 20% in 25 micron sieve. There is negligible amount of weight percentage in the pan (<25 micron). When ball milling time was increased to two hour (fig 4.3(b)), the particle size was decreased. The sieve of 90 micron size contains near about 5% weight, which was 31 % after one hour milling. The maximum weight fraction was observed between 75- 45 micron near about 40% and 45-25 micron sieve contain near to 50 % of weight. The pan (<25 micron) contains 3 % of weight.

Further increasing the milling time to three hours, the sieve of 90 micron size contains 1% weight of powder and the sieve of 75 micron size contain negligible amount of powder. The 45 micron sieve has near about 32%. The maximum powder was remained in the size between 45- 25 micron which was nearly 60 % of the total weight. A little increase in powder size below 25 micron i.e. 6 % was also observed. With the four hour milling time, the 90 % of the powder weight was between 75- 25 micron range. However the weight fraction of powder size below 25 micron remain constant, which suggest that ball milling time more than 2 two hours has no impact on the powder size below 25 microns.

Table 4.2: The comparative weight fractions of powders subjected to different milling time.

Size range	Milling time (hours)			
	1	2	3	4
>90	31.5 %	4.9 %	1.0 %	.3 %
90-75	14.8 %	1.8 %	.4 %	5.7 %
75-45	33.5 %	40.3 %	32.8 %	44.6 %
45-25	19.8 %	49.6 %	59.8 %	43.4 %
<25	.3 %	3.4 %	6.0 %	5.9 %

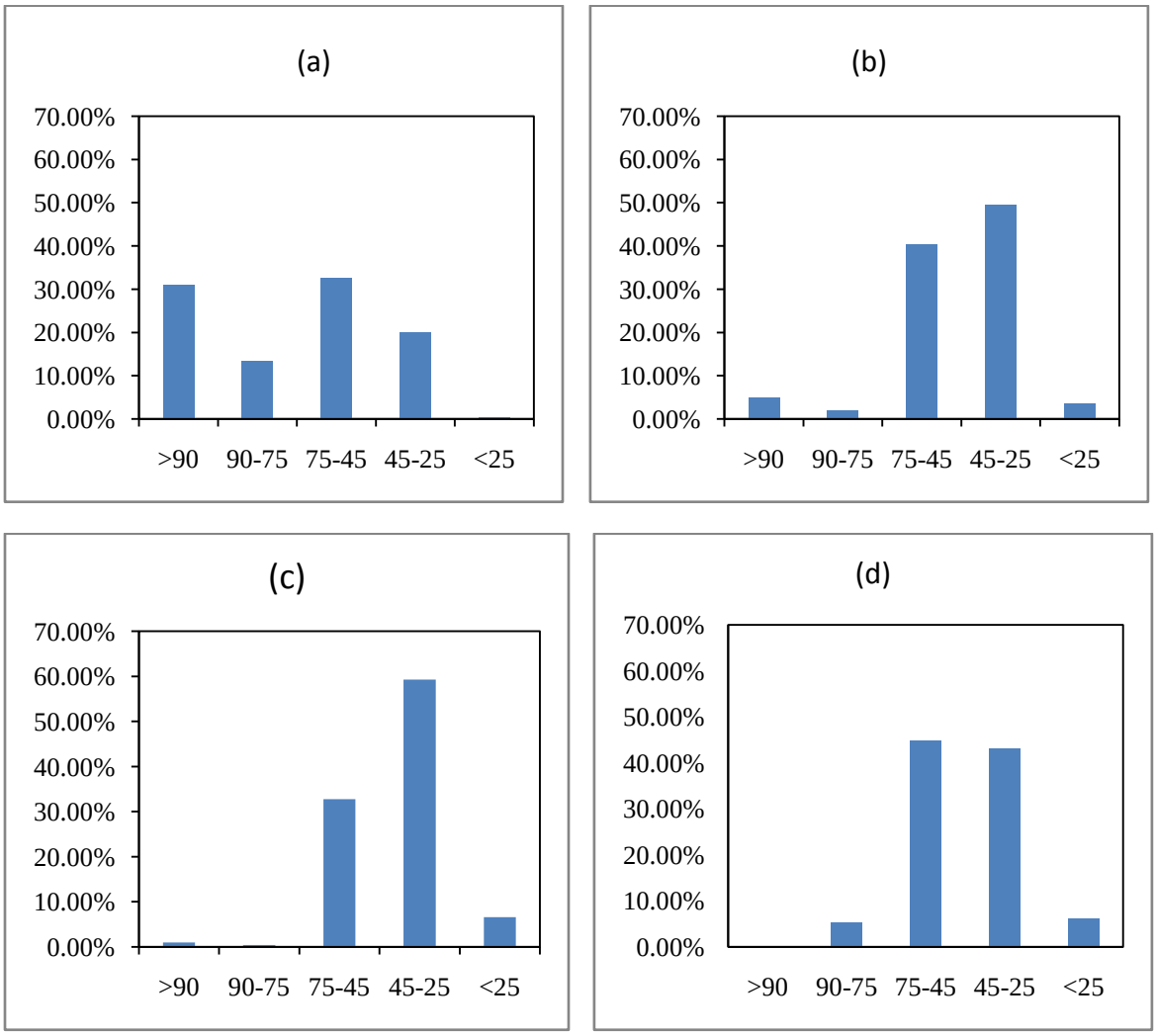

Fig. 4.3 Weight percentage of barium hexaferrite powder after (a) 1 h (b) 2 h (c) 3 h (d) 4 h ball milling.

4.3 SEM Analysis

Figure 4.4 (a, b) shows the SEM micrograph of barium hexaferrite, milled for 1 hour and 3 hours respectively. The shape of most of the particles is hexagonal and elongated, which is attributed to its hexagonal structure with largest c/a ratio. The particles which appear bigger in size are due to agglomeration of some small particles. It is also visible from the micrograph that the powder milled for three are smaller in size. The particle size analysis was carried out on SEM micrograph by counting the particle on lines drawn over to micrograph. The sizes of nearly 100 particles were measured and their particle size distribution was determined.

The figure 4.5 shows the particle size distribution calculated for 1 h and 3 h milling powders. After 1 hour milling has 13.6 % particles in the range of 0.2 to 0.4 μm particle size while the percentage of particles increases to 31.5% in the same range after 3 hours milling. The percentage of particles from 0.6 μm to 0.8 μm particle size is nearly same (approx. 48 %) for both 1 hour milling and 3 hours milling. From 1μm to 1.2 μm particle size range 1 hour milled powder has 27.3 % particles and 3 hours milled powder has 15.3 % particles. 1 hour milled powder has 10.2 % particles from the particle size range of 1.4 to 1.6 μm and 3 hours milled powder has 5.4 % particles for the same particle size range.

This is clear from the graph that the percentage of larger particle is more for 1 hour milled powder and the percentage of smaller particles is more for 3 hours milled powder. The average particle size for 1 h and 3 h was 0.7 μm and 0.5 μm respectively.

The results of particle size distribution for from sieve analysis are not in agreement with SEM. It is due to the fact that particles are agglomerated and sieve shaker could not be able to disperse the particles. However, the high magnification of SEM shows individual particles.

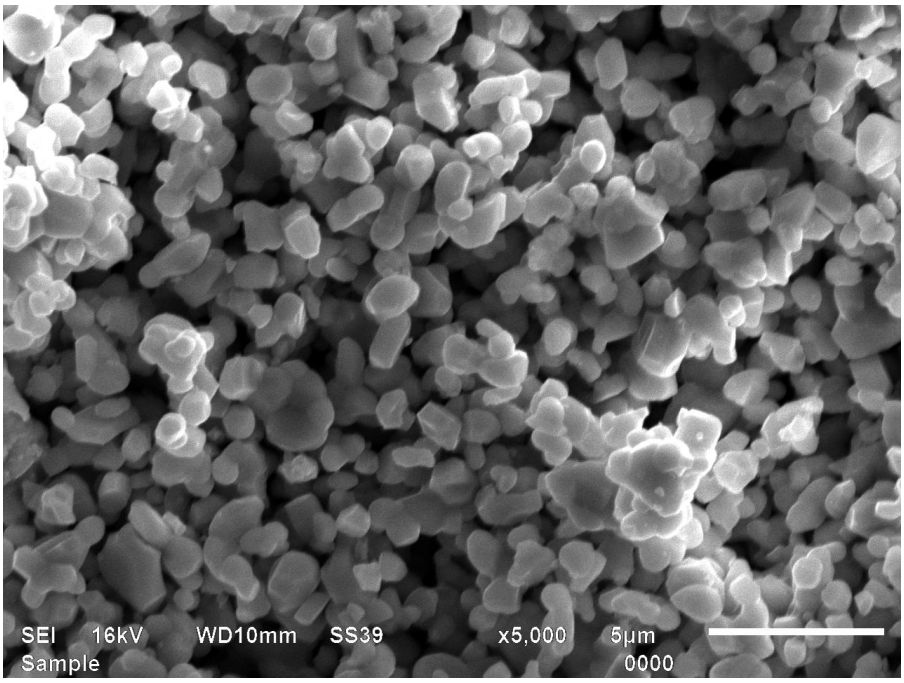

(a)

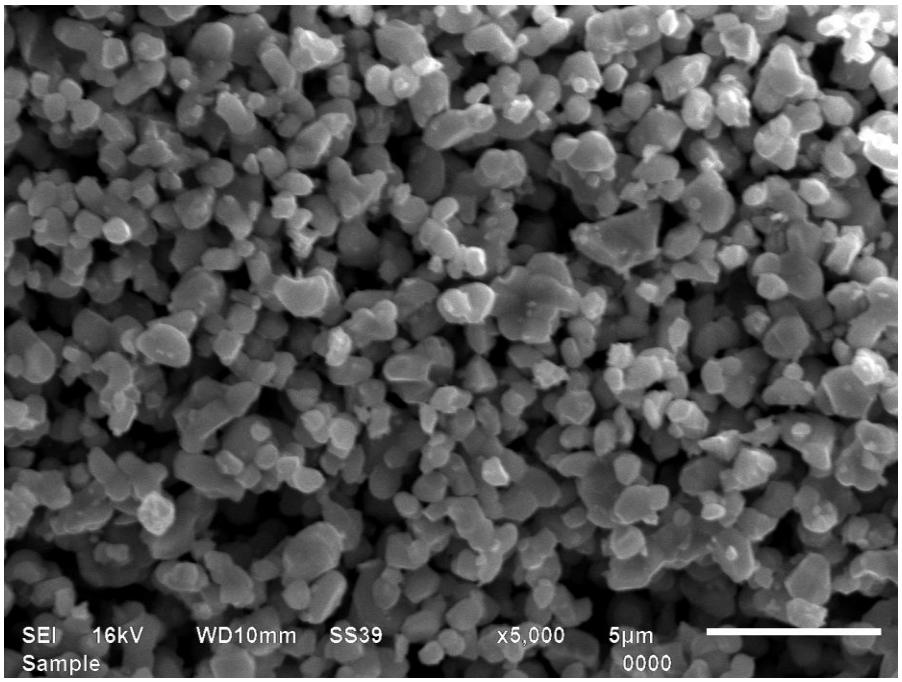

(b)

Figure 4.4: SEM micrographs of Barium hexaferrite powder (a) 1 h (b) 3h milling.

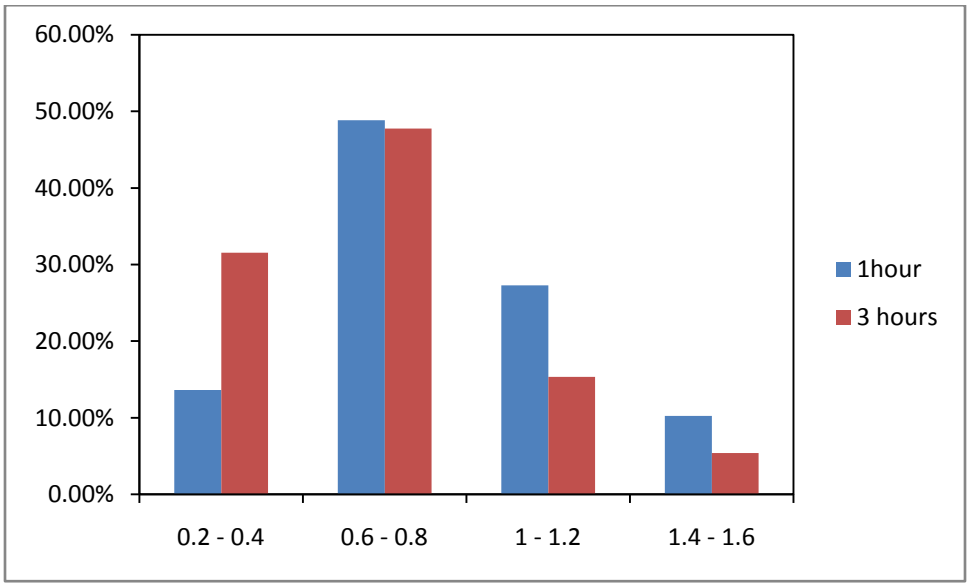

Figure 4.5: Particle size distribution of barium hexaferrite powder after 1 hour and 3 hours milling calculated from SEM micrographs.

4.4 Magnetic measurements

Magnetic measurements of the bonded magnets made from 1 h, 2 h, 3h and 4h ball milled powder were carried out by vibrating sample magnetometer (VSM). The maximum applied field was 1Tesla the step of 200 Oe.

Figure 4.7 (a, b, c and d) shows the *M-H* behavior of barium hexaferrite bonded magnets with different particle size. The values of saturation magnetization (M_s) and coercivity (H_c) measured from the graph. The coercivity bonded magnet made with 1 h ball milled was 1652 Oe which was increased to 2084 Oe bonded magnet with 4 h milled powder. This increase in coercivity is attributed to small particle size as compared to 1 h ball milled powder. In the previous work it is reported that particle size plays an important role in governing the coercivity [40]. Figure 4.7 shows the variation in coericivity with respect to milling time. The graph shows that the coericivity increases from 1652 to 2036 when the milling time increases from 1 hr to 2 h, after that very small increase in coercivity is observed. Table 4.3 shows the value of coericivity, saturation magnetization and remanent magnetization of barium

hexaferrite bonded magnets at different milling time. The values saturation magnetization and M_r remain same at different milling time.

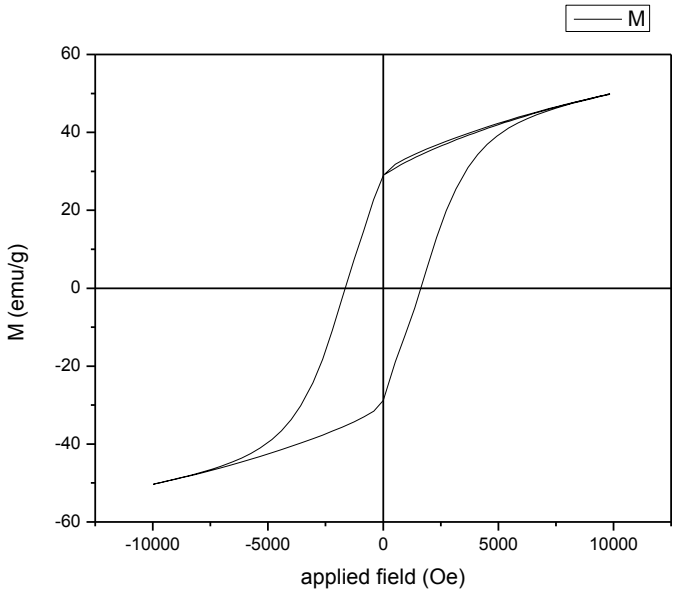

(a)

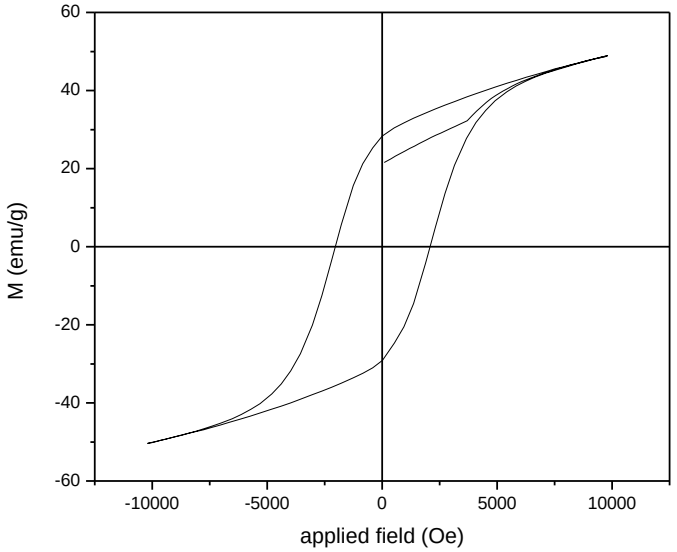

(b)

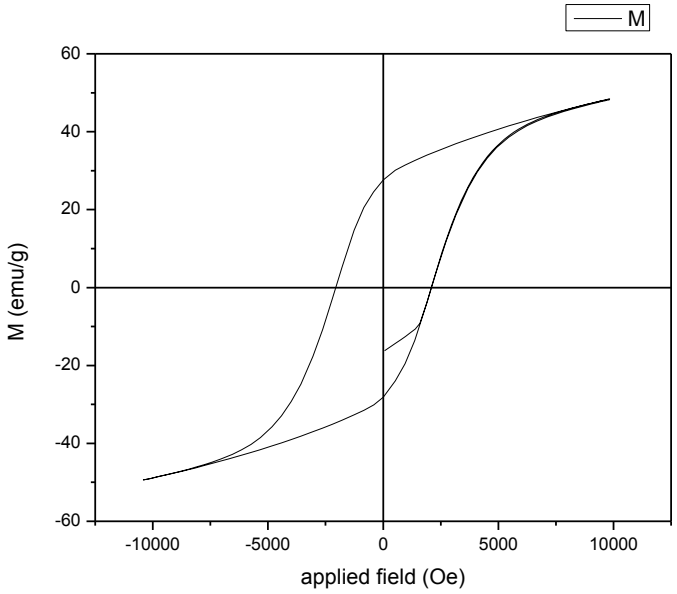

(c)

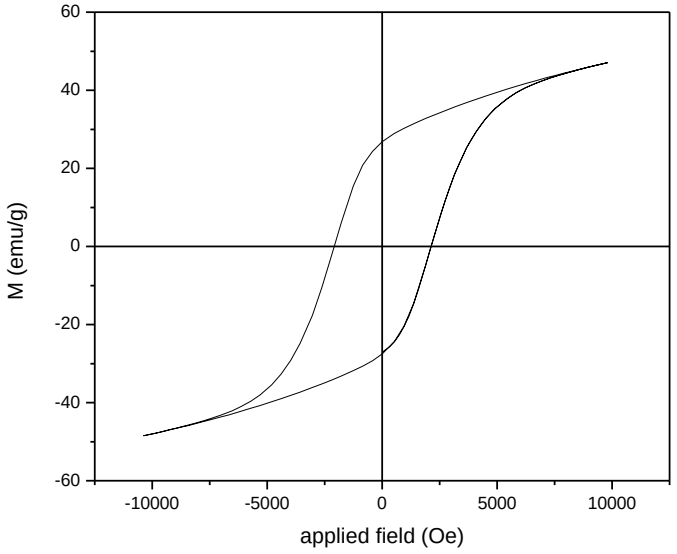

(d)

Figure 4.6 M-H behavior of barium hexaferrite milled after (a) 1 h (b) 2 h (c) 3 h (d) 4 h milling.

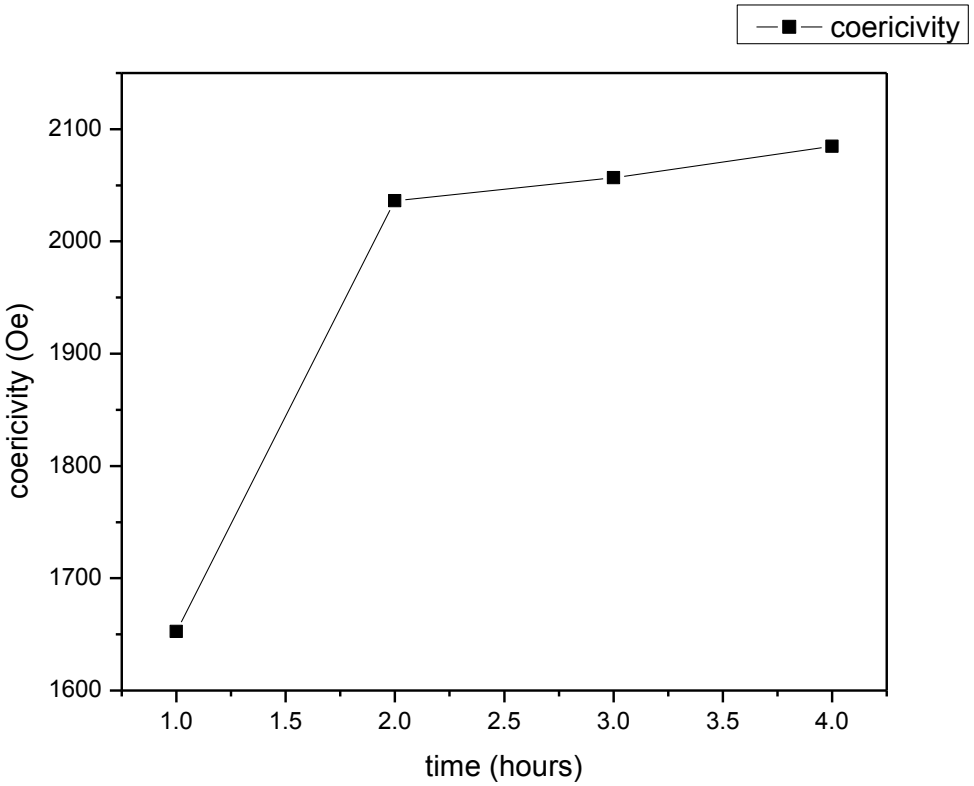

Fig. 4.7 Variation in coericivity at different milling hours

Table 4.3 Coericivity , saturation magnetization and M_r at different milling hours

Time (hrs)	Coericivity H_c (Oe)	Saturation magnetization, M_s (emu/g)	Remanent magnetization, M_r (emu/g)
1	1652	49.9	29.1
2	2036	49.1	28.8
3	2057	48.4	27.6
4	2085	46.7	26.8

Conclusion

The main focus of the present work is to prepare bonded magnets of barium hexaferrite for technological applications. Barium hexaferrite powders were prepared by solid state synthesis method. The calcination temperature and time was 1200°C and 3 h respectively. The XRD patterns show that the single barium hexaferrite phase formed. The particle size analysis was carried out by the sieve shaker and also from SEM micrographs. There is large difference is found in the particle size distribution from sieve shaker and SEM analysis. The range of particles size analyzed from SEM micrographs is from .7 μm to .5 μm while in sieve shaker it is from 90 μm to 25 μm. This is due to the fact that during vibration of the sieves the particles agglomerate with each other and due to this they do not pass through the sieves. It is found that the particle size of the prepared powder decreases as we increase the milling time. The shape of the most of the particles is hexagonal shown by SEM micrographs. From VSM analysis it is found that as the milling time increases the value of coercivity was increased from 1652.48 to 2084.79 Oe without any change in saturation magnetization.

References

1. A.J. Dekker, Electrical Engineering Materials, Prentice-Hall, (1959).

2. C.W. Chen, Magnetism and Metallurgy of Magnetic materials, North Holland Publishing Company, (1997).

3. W.H. Yeadon & A. W. Yeadon, Handbook of small Electric Motors, McGraw Hill Company Inc. USA, (2001).

4. S. Hirosawa, A. Hanaki, H. Tomizawa and A.Hamamur, Physica B. vol. 164, (1990) 117-123.

5. J.D. Livingston, A review of coercivity mechanisms, J. Appl. Phys. (1981) 522-541.

6. Min Chen and David E. Nikles, Nano Lett. (2002) 211–214.

7. F.X.N.M Kools and D. Stoppels, Kirk-Othmer Encyclopedia of Chem. Tech., Fourth Edition10, (1993) 381-413.

8. www.meder.com.

9. F.X.N.M Kools and D. Stoppels, Kirk-Othmer Encyclopedia of Chem. Tech., Fourth Edition10, (1993) 381-413.

10. S.R. Janasi, D. Rodrigues, F.J.G. Landgraf, M. Emura, IEEE Trans. Magn. 36, (2000) 3327–3329.

11. L. Lechevallier, J.M. Le Breton, J. Magn. Magn. Mater. 290–291, (2005) 1237–1239.

12. L. Lechevallier, J.M. Le Breton, J.F. Wang, I.R. Harris, J. Magn. Magn. Mater. 269, (2004) 192– 196.

13. Y. Goto and K. Takahashi, J. of Jap. Soc. Powder Metallurgy. 17, (1971) 193- 197.

14. P.B. Braun, Philips Res. Rep. 12, (1957) 491-494.

15. F. Kamamaru, M. Shimada and M. Koizumi, J. Phy. Chem. Sol. 33, (1972).

16. E.W. Gorter, 1957, Proceeding IEEE. 104B, (1957) 2255-2257.

17. J. Beretka and M. Ridge, J. Chemical Society (A). (1968) 2463-2465.

18. Patnaik, P. Dean's Analytical Chemistry Handbook, 2nd ed. McGraw- Hill, (2004).

19. Harvey, D. Modern Analytical Chemistry. McGraw-Hill, (2000).

20. www.shibang-china.com.

21. A.H. Lu, E.L. Salabas and F. Schüth, Angew. Chem., Int. Ed. (2007), 1222-1244.

22. Brinker, C.J., G.W. Scherer, Academic Press. (1990), 675-695.

23. Hench, L.L., J.K. West, Chemical Reviews. (1990).

24. Ali Ghasemi, Ardeshir Hossienpour, Akimitsu Morisako, Xiaoxi Liu, Azadeh Ashrafizadeh, Materials and Design 29. (2008) 112–117.

25. Tzu-Hao Ting, Kuo-Hui Wu, Journal of Magnetism and Magnetic Materials. 322,(2010) 2160–2166.

26. S.M. Abbas, A.K. Dixit, R. Chatterjee, T.C. Goel, Journal of Magnetism and Magnetic Materials. 309, (2007) 20–24.

27. S.P. Gairola, Vivek Verma, A. Singh, L.P. Purohit, R.K. Kotnala, Solid State Communications. 150,(2010) 147-151.

28. Zhang Haijun, Liu Zhichao, Ma Chengliang, Yao Xi, Zhang Liangying, Wu Mingzhong, Materials Science and Engineering. B96, (2002) 289-295.

29. P. Sharma, R.A. Rocha, S.N. de Medeiros, A. Paesano Jr., Journal of Alloys and Compounds. 443, (2007) 37–42.

30. Mohsen Q, Journal of alloys and compounds. 500, (2010) 125-128.

31. V. Babu, P. Padaikathan, Journal of Magnetism and Magnetic Materials. 241,(2002) 85–88.

32. P. Sharma, R. A. Rocha, S. N. de Medeiros, A. Paesano Jr & B. Hallouche Hyperfine Interact. 175, (2007) 77–84.

33. Huseyin Sozeri, Journal of Alloys and Compounds. 486, (2009) 809–814.

34. Silvia E. Jacobo, Leonardo Civale, Miguel A. Blesa, Journal of Magnetism and Magnetic Materials. 260, (2003) 37–41.

35. Koichi haneda, Choji miyakawa, Hiroshi kojima, Journal of the American Ceramic Society (1974) 354–357.

36. J.M. Soaresa, F.L.A. Machadob,_, J.H. de Arau´ joc, F.A.O. Cabralc, M.F. Ginani, Journal of Magnetism and Magnetic Materials. 310, (2007) 2529–2531.

37. I.Bsoul, S.H. Mahmoob, Journal of Alloys and Compounds 489 (2010), 110–114.

38. N.W.K, Ding J, Chow YY, Wang S, Shi Y, journal of materials research 15, (2000), 2151- 2156.

39. P. Sharma, R.A. Rocha, S.N. Mederios, B. Hallouche, A. Paesano Jr., Journal of Magnetism and Magnetic Materials 316, (2007), 29-33.

40. P. Sharma, A. Verma, R.K. Sidhu, O.P. Pandey, Journal of Magnetism and Magnetic Materials 307, (2006), 157-164.